New Solution Route to Electrochromic Poly(acrylic acid)/WO_3 Hybrid Film

Jin-Ho Choy,*,† Young-Il Kim,† Bae-Whan Kim,† Nam-Gyu Park,‡ Guy Campet,‡ and Jean-Claude Grenier‡

National Nanohybrid Materials Laboratory (NNML), School of Chemistry and Molecular Engineering, Seoul National University, Seoul 151-747, Korea, and Institut de Chimie de la Matière Condensée de Bordeaux (ICMCB), Pessac 33608, France

Received November 9, 1999. Revised Manuscript Received June 15, 2000

Electrochromic tungsten oxide film was fabricated by a new soft chemistry route, in which the transparent conducting glass substrate was successively dip-coated with poly(acrylic acid) (PAA) and ammonium tungstate solutions. The as-coated composite layer of PAA/$(NH_4)_2$-$WO_4 \cdot nH_2O$ was dried at a low temperature (100 °C), and the ammonium tungstate component was polycondensed by acid treatment in 1 N HCl to form an electrochromic PAA/WO_3 film. Transmission electron microscopy showed that the PAA/WO_3 film contains regularly dispersed WO_3 grains with an average size of ∼5 nm. According to the Auger depth profile analysis, the relative content of W, O, and C was quite homogeneous along the height of film. Depending on the concentration of PAA coating solution (1.0−3.0 wt %), the thickness and tungsten oxide content of the film were found to vary; therefore, the electrode property of the PAA/WO_3 layer could easily be controlled. By using a 2.5 wt % PAA solution, an optimum electrochromic function was achieved with a coloration efficiency of ∼38 cm^2/C and a cycle life of >11 000 under operation with $Q = 12.5$ mC/cm^2.

Introduction

Electrochromic materials undergo reversible color change through the electrochemical redox reaction, which generally is accompanied by the insertion−deinsertion of small cations: H^+, Li^+, Na^+ or K^+.[1,2] Such a property can be of considerable interest due to its applicability to various optical devices such as information displays, light shutters, smart windows, variable-reflectance mirrors, etc. Owing to its intense and stable electrochromic property, the WO_3 film has been by far the most extensively studied[3−15] with various deposition techniques such as evaporation,[6,7] sputtering,[8−10] anodic oxidation,[11] electrodeposition,[12] and sol−gel routes.[13−23] Among them, wet-chemical coating methods have recently been attracting much attention due to their advantages not only with regard to the savings in time and cost but also in respect to the large area coating. The key feature of sol−gel coating is that it presents the opportunity to control the structure of the final film at the very beginning of the process, i.e., in the preparation of the initial coating solution.[24] Since the film microstructure depends on the size and extent of aggregation of the solute species, it can be optimized by adjusting solution conditions such as pH, concentration, counterion presence, and temperature.

Although numerous attempts have been made to improve the electrochromic property of WO_3 film by controlling microstructure and composition, all of the previous sol solutions for WO_3 film have been reported

* To whom all correspondence should be addressed. Telephone: (+82) 2-880-6658. Fax: (+82) 2-872-9864. E-mail: jhchoy@plaza.snu.ac.kr.

† Seoul National University.

‡ Institut de Chimie de la Matière Condensée de Bordeaux.

(1) Monk, P. M. S.; Mortimer, R. J.; Rosseinsky, D. R. *Electrochromism, Fundamentals and Applications*; V. C. H.: New York, 1995.

(2) Granqvist, C. G. *Handbook of Inorganic Electrochromic Materials*; Elsevier Science: Amsterdam, 1995.

(3) Choy, J.-H.; Kim, Y.-I.; Kim, B.-W.; Campet, G.; Portier, J.; Huong, P. V. *J. Solid State Chem.* **1999**, *142*, 368.

(4) Choy, J.-H.; Kim, Y.-I.; Choy, S.-H.; Park, N.-G.; Campet, G.; Portier, J. In *Electrochromic Materials and Their Applications III*; Ho, K.-C., Greenberg, C. B., MacArthur, D. M., Eds.; The Electrochemical Society Proceedings Series PV 96−24; San Antonio, TX, 1997; p 303.

(5) Bange, K. *Sol. Energy Mater. Sol. Cells* **1999**, *58*, 1.

(6) Arnoldussen, T. C. *J. Electrochem. Soc.* **1981**, *128*, 117.

(7) Shiyanovskaya, I.; Hepel, M. *J. Electrochem. Soc.* **1998**, *145*, 1023.

(8) Rafla-Yuan, H.; Mathew, J. G. H.; Hichwa, B. P. *J. Electrochem. Soc.* **1996**, *143*, 2341.

(9) Batchelor, R. A.; Burdis, M. S.; Siddle, J. R. *J. Electrochem. Soc.* **1996**, *143*, 1050.

(10) Rönnow, D.; Kullman, L.; Granqvist, C. G. *J. Appl. Phys.* **1996**, *80*, 423.

(11) Ord, J. L.; De Smet, D. J. *J. Electrochem. Soc.* **1992**, *139*, 728.

(12) Meullenkamp, E. A. *J. Electrochem. Soc.* **1997**, *144*, 1664.

(13) Chemseddine, A. *J. Non-Cryst. Solids* **1992**, *147−148*, 313.

(14) Judeinstein, P.; Livage, J. *J. Mater. Chem.* **1991**, *1*, 621.

(15) Yamanaka, K.; Okamoto, H.; Kidou, H.; Kudo, T. *Jpn. J. Appl. Phys.* **1986**, *25*, 1420.

(16) Sbar, N.; Badding, M.; Budziak, R.; Cortez, K.; Laby, L.; Michalski, L.; Ngo, T.; Schulz, S.; Urbanik, K. *Sol. Energy Mater. Sol. Cells* **1999**, *56*, 321.

(17) Ozer, N.; Lampert, C. M. *Thin Solid Films* **1999**, *349*, 205.

(18) Klisch, M. *J. Sol-Gel Sci. Technol.* **1998**, *12*, 21.

(19) Cronin, J. P.; Tarico, D. J.; Agrawal, A.; Zhang, R. L. U.S. Patent 5,277,986 Jan. 11, 1994.

(20) Antinucci, M.; Chevalier, B.; Ferriolo, A. *Sol. Energy Mater. Sol. Cells* **1995**, *39*, 271.

(21) Azens, A.; Hjelm, A.; Le Bellac, D.; Granqvist, C. G.; Barczynska, J.; Pentjuss, E. *Solid State Ionics* **1996**, *86−88*, 943.

(22) Borissevitch, A. Yu.; Yanovskaya, M. I.; Kessler, V. G.; Nikonorova, N. I. *J. Sol-Gel Sci. Technol.* **1998**, *12*, 111.

(23) Klisch, M. *J. Sol-Gel Sci. Technol.* **1998**, *12*, 21.

(24) Brinker, C. J.; Scherer, G. W. *Sol−Gel Science: The Physics and Chemistry of Sol−Gel Processing*; Academic: London, 1990; chap 13.

10.1021/cm990718h CCC: $19.00
Published on Web 09/15/2000

only in acidic media, with acidification of an aqueous salt (Na_2WO_4 or K_2WO_4),[13] hydrolysis of chloroalkoxide,[14] and dissolution of tungsten metal in H_2O_2 solution.[15−23] On the basis of the solubility phase diagram for the tungstate species, we could predict that all of these acidic solutions are dominated by polynuclear tungstate ions[25] and that such larger parent species may readily form compact and extended oxide networks. On the other hand, if smaller solute precursors are used for the WO_3 coating, the microstructure of film can be controlled more freely toward the desirable electrochromic performance. In the electrodes of electrochromic or battery-type devices, their electrochemical activity is closely associated with intercalation property. In particular, it is of great interest to fabricate electrode materials in the nanocrystalline form, since they can provide abundant and easily accessible redox sites owing to the large surface area. In this regard, we became interested in the preparation of a new coating solution for WO_3 film which would be completely different from an acidic solution. As tungsten oxide is soluble in a hot basic medium, a basic precursor solution could be prepared for WO_3 film. In contrast to an acidic solution, in which polynuclear tungstate ions are dominant, smaller mononuclear ions such as WO_4^{2-} are stabilized mainly in a basic solution as predicted from the pC_i versus pH diagram. In the present study, an attempt was made to prepare a new coating solution for electrochromic film and to correlate the electrochromic property with its microstructure.

Recently, we have been able to fabricate an electrochromic hybrid film of polymer/WO_3 by performing the dip coating on tin-doped indium oxide (ITO) glass with poly(acrylic acid) (PAA) and ammonium tungstate solutions, successively,[3,4,26] and the PAA/WO_3 film thus obtained was highly transparent with a marked electrochromic property. In this study, it is also demonstrated how the PAA/WO_3 film is formed with a homogeneous hybrid structure in which the PAA provides a porous matrix for the electrochromic tungsten oxide grains. In addition, the electrochemi-optical behavior of this hybrid film is quantitatively investigated in relation to the concentration of PAA coating solution.

Experimental Section

The electrochromic hybrid film was prepared on ITO glass by successive dip-coatings in PAA−EtOH and WO_3−ammonia water solutions. The PAA (Aldrich, $M_v \approx 450\,000$) was dissolved in absolute EtOH (Hayman, 99.9%) with concentrations of 1.0, 1.5, 2.0, 2.5, and 3.0 wt % by stirring for 6 h at room temperature. The viscosity of PAA solution changed from 5 to 16 cP depending on the concentration. The basic solution was prepared by dissolving 7 g of WO_3 (Aldrich, 99+%) powder in 40 mL of boiling ammonia solution (15%), and then by adding 60 mL of deionized water to it. The resulting solution was stirred for 24 h at room temperature and filtered before use.

A pre-cleaned ITO substrate glass (Samsung Corning, 15 Ω/sq., size 10 × 10 cm^2) was dipped into PAA solution, withdrawn with a rate of 16 cm/min, and dried at 80 °C for 10 min. The PAA layer was dip-coated again with WO_3−ammonia water solution with the same withdrawal speed and dried at 100 °C for 10 min. Then, the PAA/ammonium tungstate film was subjected to a galvanostatic reduction−oxidation cycle in 1 N HCl with a charge density of 10 mC/cm^2 to remove the ammonium species. The above acid-treated film was rinsed with absolute EtOH and dried at a reduced pressure ($P \approx 10^{-3}$ Torr) for 1 h.

The thickness of each PAA layer and the PAA/WO_3 one was measured by scanning electron microscopy (SEM; JEOL, JSM-840A) and surface profilometry (Talyor Hobson, Talystep). The grain morphology of the film was observed with transmission electron microscopy (TEM; JEOL, 2000FX). For TEM measurements, the powdered sample was prepared by scratching the film surface with a steel blade. Inductively coupled plasma spectroscopy (ICP; Philips, ARL 3580) was employed to determine the concentration of tungsten in each film. The depth profile was recorded for W, C, N, In, and O by performing Auger electron spectroscopy[27] (AES; VG Scientific, VG 310F), and for the calculation of atomic concentrations, five lines of W NO_1, C KL_1, N KL_1, In MN_1, and O KL_1 were selected at 166.00, 267.31, 384.97, 404.99, and 525.00 eV, respectively. The chemical state of tungstate species films was probed also by vibrational spectroscopy. The Fourier transform infrared (FT-IR; Nicolet 740) spectra were collected in the reflective mode, and the micro-Raman measurements were performed using a LABRAM spectrometer (Jovin Yvon-Spex-Dilor) with an Ar ion laser (Spectra Physics).

Electrochemical and optical measurements were carried out with an automatically controlled potentiostat/galvanostat (Radiometer Copenhagen, PGP 201) and a UV−visible spectrophotometer (Varian Cary 2415). For the working electrode, each film was processed to have an active area of 1.2 cm^2, and the Pt wire and Ag/AgCl with Luggin capillary were used as counter and reference electrodes, respectively. The lithium electrolyte was prepared by mixing 10 wt % of $Li(CF_3SO_2)_2N$ (LiTFSI) with the hydrophobic molten salt, 1,3-EtMeIm$(CF_3SO_2)_2N$ (EtMeImTFSI),[28,29] in the N_2-filled drybox. Cyclic voltammetry for PAA/WO_3 film was performed in the potential (E) range −0.8 to ca. +0.5 V (vs Ag/AgCl) with a sweep rate of 5 mV/s. The electrochromic property of the film was evaluated after 30 cycles of voltammetric sweeping. The transmittance (T) of the film was monitored at $\lambda = 550$ nm, upon the electrochemical injection/extraction of Li^+, where a constant current of $j = 50\ \mu A/cm^2$ was applied up to a charge density of $Q = 12.5$ mC/cm^2. A long-term durability test was carried out in the galvanostatic charge−discharge mode ($j = 250\ \mu A/cm^2$, $Q_{max} = 12.5$ mC/cm^2) during which the film's electrochromic function was measured after every 500 cycles.

Results and Discussion

In this study, the concentration of PAA coating solution was varied as 1.0, 1.5, 2.0, 2.5, and 3.0 wt %, and hereafter, the corresponding PAA/WO_3 films will be denoted as P10W, P15W, P20W, P25W, and P30W, respectively. After each step of PAA coating and subsequent WO_3 coating, the film thickness was measured by SEM and surface profilometry. In accordance with the general relation between film thickness and viscosity of the coating solution,[24] the PAA layer became thicker upon increasing the concentration of PAA solution. On the other hand, the thickness of the PAA/WO_3 layer was nearly the same as that of PAA for all five specimens. Moreover, the cross-sectional SEM view of the PAA/WO_3 films (Figure 1) indicates that there is no discrete boundary between PAA and WO_3. These results imply that the PAA/WO_3 film is formed not by

(25) Baes, C. F., Jr.; Mesmer, R. E. *The Hydrolysis of Cations*; Wiley-Interscience, New York, 1976; p 257.
(26) Park, N.-G.; Kim, B.-W.; Poquet, A.; Campet, G.; Portier, J.; Choy, J.-H.; Kim, Y.-I. *Active Passive Elec. Components* **1998**, *20*, 125.
(27) Ohring, M. *The Materials Science of Thin Films*; Academic: San Diego, 1991; pp 275−278.
(28) Bonhôte, P.; Dias, A.-P.; Papageorgiou, N.; Kalyanasundaram, K.; Grätzel, M. *Inorg. Chem.* **1996**, *35*, 1168.
(29) Park, N.-G.; Poquet, A.; Campet, G.; Portier, J.; Choy, J.-H.; Kim, Y.-I.; Camino, D.; Salardenne, J. *Active Passive Elec. Components* **1998**, *20*, 201.

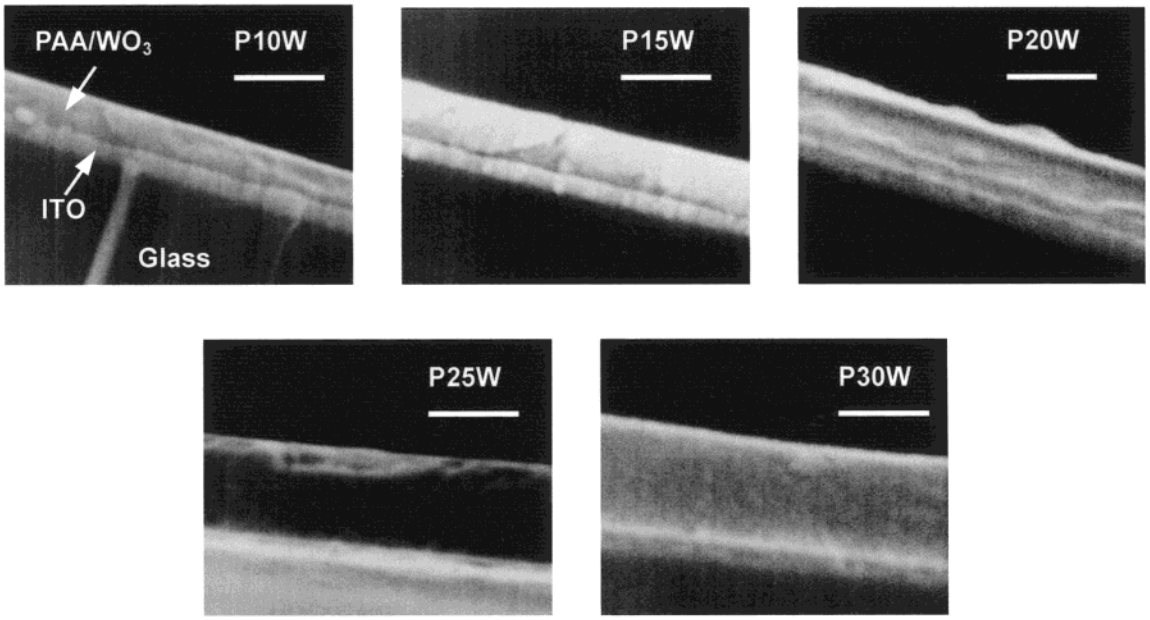

Figure 1. Cross-sectional SEM photographs for PAA/WO_3 hybrid films prepared from PAA solutions with different concentrations: 1.0% (P10W), 1.5% (P15W), 2.0% (P20W), 2.5% (P25W), and 3.0% (P30W). Each scale bar corresponds to 1 μm (magnification, 20K).

Table 1. Thickness and Tungsten Concentration of the PAA/WO_3 Films

		C_W[b]		
sample	t (μm)[a]	(mg/cm^2)[c]	(μmol/cm^2)[d]	(mmol/cm^3)[e]
P10W	0.38(2)	0.083_5	0.45_4	$12._0$
P15W	0.55(1)	0.13_4	0.72_7	$13._2$
P20W	0.70(2)	0.16_7	0.90_8	$13._0$
P25W	1.16(2)	0.18_4	1.0_0	8.6_2
P30W	1.20(2)	0.22_4	1.2_2	$10._2$

[a] Thickness of PAA/WO_3 film measured by SEM. [b] Concentration of W in the film. [c] Mass concentration of W determined by ICP. [d] Molar concentration of W per unit area. [e] Molar concentration of W per unit volume. For comparison, C_W for bulk WO_3 (monoclinic) is 32.1 mmol/cm^3.

layer-by-layer stratification but by homogeneous mixing to a nanohybrid consisting of PAA and tungstate, where the PAA layer serves as a permeable matrix for the WO_3 coating solution. The thickness of the PAA/WO_3 layer and the concentration of tungsten in each film are summarized in Table 1, showing that both parameters increase almost linearly with respect to the concentration of PAA coating solution.

To confirm the hybrid structure of PAA/WO_3 films and to examine the effect of acid treatment, the AES depth profiles of W, O, C, N, and In were recorded for P10W−P30W. Figure 2a,b demonstrates the change of internal composition in P10W before and after the H^+ treatment, where it is readily recognized that the ammonium components are effectively removed by the H^+ treatment. In addition, it is worthwhile to note here that the W and C concentrations are almost constant from the film surface to the bottom, indicating that the WO_3 domains are homogeneously distributed over the PAA medium. Similar composition distributions were also observed for P20W (Figure 2c) and P30W (Figure 2d) together with increase of the film thickness in accordance with the SEM analysis.

The FT-IR and micro-Raman analyses were performed to investigate the evolution of chemical phases occurring in the formation process of PAA/WO_3 film.

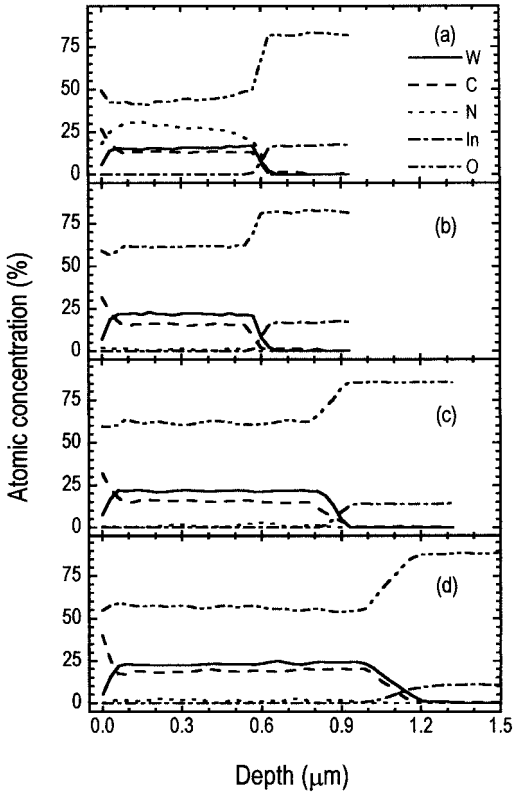

Figure 2. Depth profiles for (a) P10W before H^+ treatment, (b) P10W, (c) P20W, and (d) P30W. Key: W, solid; C, dash; N, dot; In, dash dot; O, dash dot dot.

Figures 3 and 4 represent the reflective FT-IR and micro-Raman spectra, respectively, for the P25W film before and after H^+ treatment. In Figure 3a, the spectrum of PAA is dominated by the peaks due to main functional groups of poly(acrylic acid). After the ammonium tungstate coating, additional peaks from WO_4^{2-}, NH_4^+, and OH^- species[30] are newly observed indicating that the tungsten species are successfully included into

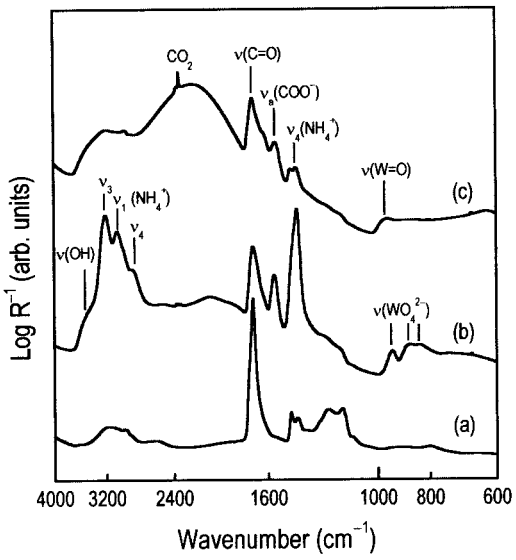

Figure 3. Reflective FT-IR spectra for PAA and PAA/WO_3 films on ITO glass: (a) PAA, (b) P25W before H^+ treatment, and (c) P25W.

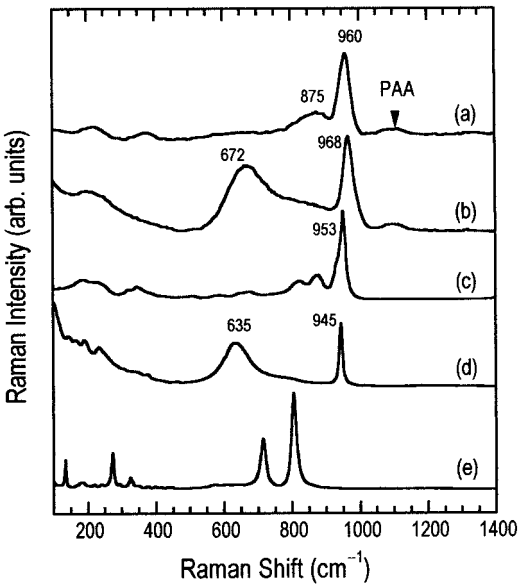

Figure 4. Micro-Raman spectra measured for PAA/WO_3 films on ITO glass, (a) P25W before H^+ treatment and (b) P25W, and powdered reference compounds, (c) $(NH_4)_2WO_4$, (d) H_2WO_4, and (e) monoclinic WO_3.

PAA media, probably as the form of ammonium tungstate hydrate. On the other hand, Figure 3c shows that H^+ treatment results in a disappearance of NH_4^+ and WO_4^{2-} species, and in the formation of W═O bonds as revealed by the spectral features at ∼960 cm^{-1}. In agreement with the FT-IR observation, the micro-Raman spectra (Figure 4) also show that a characteristic vibration mode of WO_4^{2-} (875 cm^{-1}) disappears upon H^+ treatment, accompanying an appearance of the stretching mode of O−W−O lattice (672 cm^{-1}). As compared in Figure 4a−d, the Raman spectra of the PAA/WO_3 film as-coated and the H^+-treated one represent overall similarities to those of $(NH_4)_2WO_4$ and H_2WO_4, respectively. Although there are slight peak shifts between parts a and c of Figure 4 and between parts b and d of Figure 4, they can be ascribed to a distinct degree of hydration or the presence of the PAA. From the above FT-IR and micro-Raman investigations, we could understand explicitly that the ammonium tungstate hydrate component in the as-coated composite layer is polycondensed to tungsten oxide hydrate through protonic exchange of ammonium ion.

The crystal structure and morphology of WO_3 in the PAA/WO_3 hybrid film were studied by TEM for which the powder sample was gathered by scratching off the P15W specimen. Figure 5a presents the TEM image of the PAA/WO_3 hybrid (magnification, 600K), where it is shown that the tungsten oxide particles are embedded in PAA media with an average diameter of ∼5 nm. Because the WO_3 crystallite in this hybrid is extremely small in size and disordered, the electron diffraction pattern (Figure 5b) could not be analyzed. However from the above image pattern, we were able to interpret an individual grain as a lamella crystallite with a layer separation of ∼3.5 Å.

On the basis of the above findings, the fabrication process of PAA/WO_3 film is described by a schematic model as illustrated in Figure 6. Since the PAA behaves as an amorphous and porous matrix for WO_3 crystallites, a uniform hybrid structure of PAA/WO_3 can be realized. It is noteworthy, in particular, that the PAA can allow the physical and electrical contacts between WO_3 component and ITO substrate, as evidenced by the Auger depth profile analysis. The sizes of WO_3 grains are spatially regulated by a polymer network, where the oxide nanoparticles are formed with a layered structure adequate for the intercalation of H^+ or Li^+. It is therefore expected that the PAA/WO_3 hybrid film will constitute a promising new electrode for electrochromic devices.

The electrochemical and electrochromic properties of the PAA/WO_3 films have been examined in a hydrophobic LiTFSI−EtMeImTFSI electrolyte with cyclic voltammetry and spectrophotometry under chronopotentiometric conditions. Figure 7 compares 30 successive cycles of voltammetry profiles measured for the five films, P10W−P30W. In all cases, the voltammograms undergo significant evolution which can be attributed to the formatting[31] (or conditioning) process of the film. Owing to the nanocrystalline nature of the oxide component, the as-prepared PAA/WO_3 film contains abundant surface defects which can be cured by repeated ion insertion−extraction processes.[32] Along with the progress of voltammetry cycles, the five samples commonly exhibited a positive shift in the coloration onset potential as well as a negative shift in the reduction peak potential. This means that the microstructure of PAA/WO_3 film is gradually modified for the faster intercalation and deintercalation of Li^+ through the formatting procedure. In cyclic voltammetry, the integrated charge (Q) can be a good indicator of the electrochemical activity of the electrode. Figure 8 shows that both the Q_{ox} and $-Q_{red}$ values increase from P10W to P25W in parallel with the tungsten content in the film (Table 1),

(30) Nyquist, R. A.; Kagel, R. O. *Infrared Spectra of Inorganic Compounds (3800−45 cm^{-1})*; Academic: San Diego, 1997; pp 344−345.

(31) The as-prepared ion-insertion electrodes are very prone to electrochemical degradation. Therefore, they should initially be subjected to charge−discharge cycles with current density lower than that of the normal operation condition (approximately on the order of a tenth).

(32) Michalak, F. M.; Owen, J. R. *Solid State Ionics* **1996**, *86*, 965.

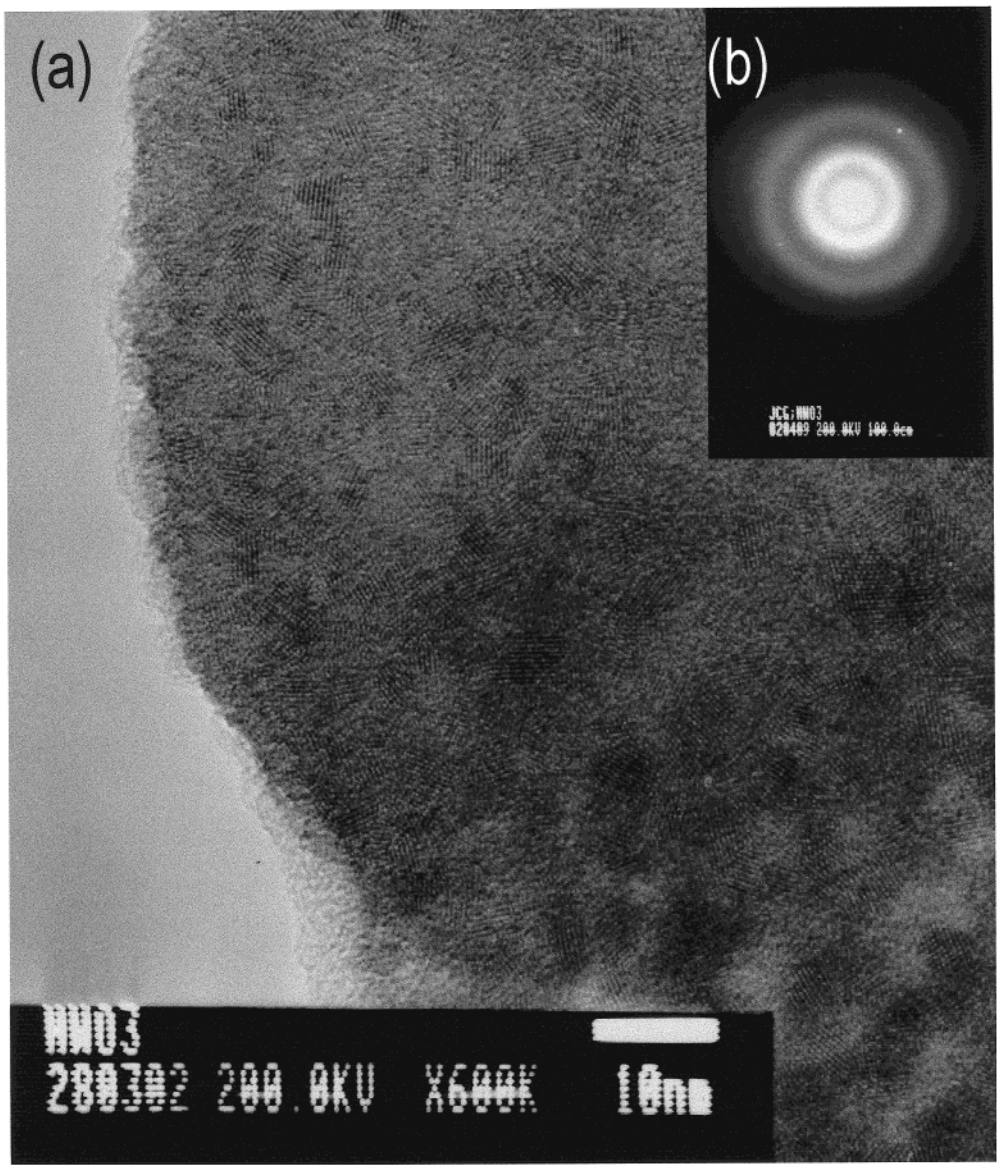

Figure 5. (a) High-resolution TEM image of the PAA/WO_3 powder sample taken from P15W specimen and (b) electron diffraction pattern. Scale bar corresponds to 10 nm (magnification, 600K).

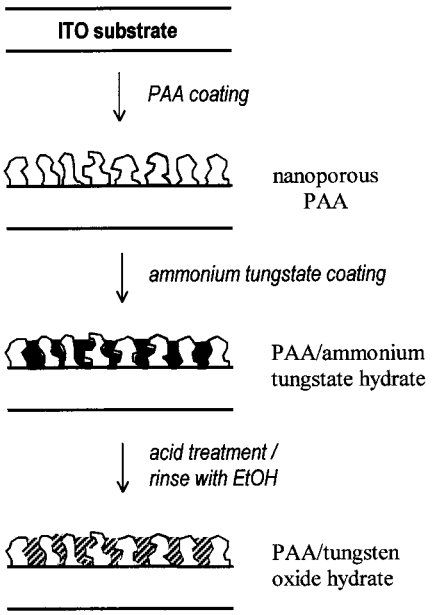

Figure 6. Preparation scheme for the PAA/WO_3 hybrid film.

while they decrease considerably from P25W to P30W. In the present fabrication method for PAA/WO_3, it is thought that the concentration of PAA solution plays a crucial role not only in the physical properties of the film, such as thickness, adhesion to the substrate, etc., but also in the electrochemical properties through the control of electrode conductivity or the chemical environment around WO_3 crystallite. The cyclic voltammetry results imply that the P25W specimen was prepared with the highest attainable electrochemical activity and most probably with the optimum electrochromic performance.

The electrochromic property of the film was evaluated after 30 cycles of voltammetric sweeping. To measure the electrochromic property of PAA/WO_3, the T of the film was monitored at $\lambda = 550$ nm during the galvanostatic Li^+ insertion−deinsertion cycle. The coloration efficiency (η) of each film could be estimated from the relation $\eta = \Delta OD/Q = [\log(T_{bleached}/T_{colored})]/Q$.[33] As is

(33) Granqvist, C. G. *Handbook of Inorganic Electrochromic Materials*; Elsevier Science: Amsterdam, 1995; p 165.

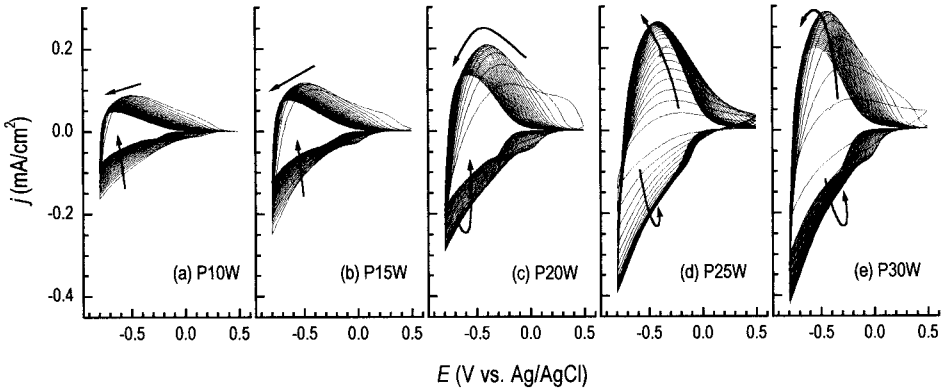

Figure 7. Cyclic voltammograms for (a) P10W, (b) P15W, (c) P20W, (d) P25W, and (e) P30W. (30 cycles).

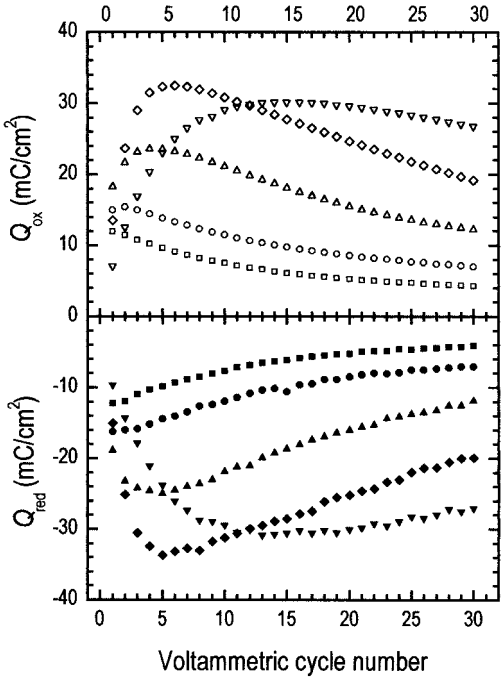

Figure 8. Exchange charges during cyclic voltammetry of Figure 7. The oxidation (Q_{ox}) and reduction charges (Q_{red}) are plotted with open and filled symbols, respectively. Key: P10W, square; P15W, circle; P20W, upward triangle; P25W, downward triangle; P30W, diamond.

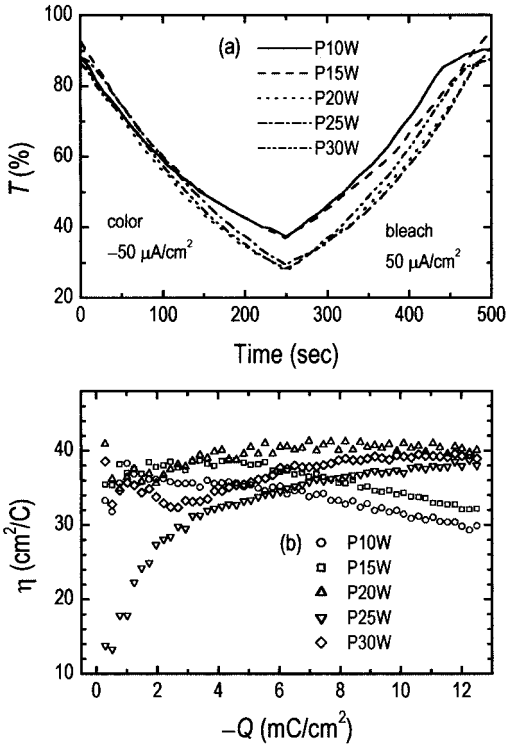

Figure 9. (a) Transmittance variation of PAA/WO_3 films during galvanostatic Li^+-insertion/extraction cycle. (Key: P10W, solid; P15W, dash; P20W, dot; P25W, dash dot; P30W, dash dot dot) and (b) coloration efficiency during charge injection process (Key: P10W, square; P15W, circle; P20W, upward triangle; P25W, downward triangle; P30W, diamond).

shown in Figure 9a, the initially colorless films become colored in accordance with the accumulation of Li^+, and they could reversibly be bleached by the reverse process. The ΔT's at $Q = 12.5$ mC/cm^2 were 51%, 56%, 60%, 59%, and 58% for P10W, P15W, P20W, P25W, and P30W, respectively. The η's of the films changed depending on the Li^+ concentration and can be regarded as the functions of Q (Figure 9b). In the vicinity of $Q \approx 5$ mC/cm^2, the η's of the five films were 32−40 cm^2/C without a clear dependence on the concentration of PAA coating solution. However, upon further lithiation, the two specimens with lowest PAA concentration, P10W and P15W, exhibited a gradual decrease of η, in contrast to the others. As stated above (Table 1), the area density of W in the film gradually decreases from P30W to P10W, so the inferior electrochromic properties of P10W and P15W could be attributed to their low charge capacity. For example, the P10W specimen was formed with a W density of 0.45_4 μmol/cm^2, and the charge insertion of 12.5 mC/cm^2 corresponds to the nominal [Li]/[W] ratio of 0.29 which is very close to the limiting value for tetragonal tungsten bronze, Li_xWO_3 ($0.01 \leq x \leq 0.36$).[34] It is therefore concluded that the coloration of P10W and P15W is saturated at a relatively lower level of charge injection. On the other hand, the specimens of P20W−P30W could maintain their stable electrochromic activities with η's of 38−40 cm^2/C at a charge density over 12.5 mC/cm^2.

The long-term durability of PAA/WO_3 films was tested by continuous charge−discharge cycles with $j = 250$ μA/cm^2 and $Q = 12.5$ mC/cm^2 (100 s/cycle). At every 500th cycle, electrochemi-optical measurements were performed, and the lifetime of the film was determined to be the point at which the ΔT during a cycle dropped to

(34) Zhong, Q.; Dahn, J. R.; Colbow, K. *Phys. Rev. B* **1992**, *46*, 2554.

half that during the initial cycle. Usually, the service lifetime of the electrochromic electrode or the complete electrochromic device can be estimated by conducting repetitive electrical cycling using the step voltages for coloring and bleaching. Such a voltage control is preferred to the current one since the former can better simulate a real operating situation and can avoid unexpected damage to the device. However, in the present preliminary durability test of PAA/WO_3 film, we have chosen a galvanostatic switching condition in order to ensure the constancy of the charge insertion level.

In the cases of P10W and P15W, the degradation of the electrochromic function occurred rapidly resulting in lifetimes shorter than 1000 cycles. However, the films prepared from the concentrated PAA solutions exhibited much better durability with 4500, 11000, and 8500 cycles for P20W, P25W, and P30W, respectively. Taking into account the fact that the present test conditions are rather severe compared to the widely proposed electrical cycling conditions,[35−37] the PAA/WO_3 hybrid is regarded as a novel electrochromic system which may even be applicable to commercial devices. The role of PAA can be emphasized here again in connection with the durability of the hybrid film. In general, amorphous and nanocrystalline oxides, as in PAA/WO_3, are lacking in physical or chemical stability, whereas they are much more reactive than their crystalline forms. In the case of the PAA/WO_3 hybrid, however, the PAA seems to act as the binderlike support endowing the electrochromic tungsten oxide nanoparticles with an improved cyclability. It is therefore necessary to examine whether the PAA participates in electrochemical reaction of the tungsten oxide by performing a future comparative study using different polymers, electrolytes, or tungstate solutions.

Conclusion

A new type of organic/inorganic hybrid film of PAA/WO_3 was developed for electrochromic systems by coating ITO glass successively with PAA and a basic solution containing monotungstate species. The TEM and AES depth profile analyses indicated that tungsten oxide crystallites are prepared with nanosized domains embedded in the PAA media and that they are distributed homogeneously over the entire film regardless of film thickness. The higher the concentration of PAA in the coating solution, the larger the area density of tungsten oxide becomes, and thereby the electrochromic function of hybrid film could be modified by adjusting the concentration of PAA coating solution. In the optimal case where the 2.5 wt % PAA solution was used, the PAA/WO_3 film exhibited voltammetric charges of $Q_{red} = -27.0$ mC/cm^2 and $Q_{ox} = 26.8$ mC/cm^2 between -0.8 and $+0.5$ V (vs Ag/AgCl), an electrochromic efficiency of $\sim$38 cm^2/C, and a greater than 11 000 times longer lifetime. In achieving the electrochromic PAA/WO_3 film, the PAA is surely an essential component that facilitates not only the formation of nanocrystalline oxide grains but also electrochromic activity and extended cyclability.

Acknowledgment. This work was supported in part by the Korea Energy Management Corporation and by the Ministry of Science and Technology through National Research Laboratory program. Y.I.K. is grateful to the Ministry of Education for the BK21 fellowship.

Supporting Information Available: Plots of transmittance versus time for P10W−P30W. This material is available free of charge via the Internet at http://pubs.acs.org.

CM990718H

(35) Hashimoto, S.; Matsuoka, H. *J. Electrochem. Soc.* **1991**, *138*, 2403.
(36) Czanderna, A. W.; Benson, D. K.; Jorgensen, G. J.; Zhang, J.-G.; Tracy, C. E.; Deb, S. K. *Sol. Energy Mater. Sol. Cells* **1999**, *56*, 419.
(37) Tracy, C. E.; Zhang, J.-G.; Benson, D. K.; Czandera, A. W.; Deb, S. K. *Electrochim. Acta* **1999**, *44*, 3195.